




Open Archive Toulouse Archive Ouverte (OATAO)

OATAO is an open access repository that collects the work of Toulouse researchers and makes it freely available over the web where possible

This is an author's version published in: <http://oatao.univ-toulouse.fr/20294>

Official URL: <https://doi.org/10.1002/elan.201400155>

To cite this version:

Koita, Démo and Tzedakis, Théo  and Kane, Cheikhou and Diaw, Mahy and Sock, Oumar and Lavedan, Pierre *Study of the Histamine Electrochemical Oxidation Catalyzed by Nickel Sulfate*. (2014) *Electroanalysis*, 26 (10). 2224-2236. ISSN 1040-0397

Any correspondence concerning this service should be sent to the repository administrator: tech-oatao@listes-diff.inp-toulouse.fr

Study of the Histamine Electrochemical Oxidation Catalyzed by Nickel Sulfate

Démo Koita,^[a] Theodore Tzedakis,^{*[b]} Cheikhou Kane,^[a] Mahy Diaw,^[a] Oumar Sock,^[a] and Pierre Lavedan^[c]

Abstract: Thin layer technique was applied to the indirect anodic oxidation of histamine, catalyzed by NiSO₄. Coulometric determination of the electron number demonstrates that histamine complexes Ni^(II) and resulting adducts can be electrochemically oxidized in a single-electron reaction, to lead Ni^(III)-histamine. The system Ni^(III)/Ni^(II) acts as 'redox mediator' for histamine oxidation.

Keywords: Histamine oxidation • Electrochemical thin layer • Nickel catalyst • Fish

1 Introduction

Histamine (C₅H₉N₃ referred to as (Hm)), like some other biologically active amines, present in fish such as tuna-fish, mackerel, sardine and so on, are responsible for food poisoning [1,2]. Toxicity can become effective for histamine concentrations in the range of 0.5 to 1 g/kg of fish.

Some other diamines such as putrescine NH₂-(CH₂)₅NH₂, cadaverine NH₂(CH₂)₄NH₂ are able to block histamine degradation in the human body and consequently to perpetuate the histamine toxicity. In addition, these amines can react with nitrites to form nitrosamines which are potential carcinogenic products [3,4]. Thus, a good factor enabling fish freshness to be characterized is its content in amines, especially histamine.

Various analytical methods have been developed to isolate and measure the content of these amines [5,6]. Nevertheless, as far as we know, there is no standard and simple analytical method to detect and to quantify these biogenic amines, extracted from food, using organic solvents or mineral acids (perchloric, trichloroacetic, hydrochloric). The analytical methods used for the separation and quantification of amines (histamine, tyramine, cadaverine, putrescine, spermidine and spermine) that are contained within the matrix, that result from the extraction of these products from food, are mainly based on chromatographic methods: gas chromatography, thin-layer and high-performance liquid chromatography (HPLC), reversed phase, with precolumn, post-column or on-column derivatization techniques [7–9]. These methods generally require functionalizing the amines employing complicated processes that last a relatively long time.

Fluorescence methods are also involved in analyzing these amines after separation; for example for detecting the histamine in the fish [10–12], the follow sequence was applied: extraction by trichloroacetic acid; separation of the interfering products using ionic exchange chromatog-

raphy; reaction of the amine on the *ortho*-phthalaldehyde (OPA), leading a to colorized solution.

Several electrochemical methods [13–24], especially pulse amperometry (PAD), sometimes using electrochemically modified electrodes (glassy carbon + films of nickel, gold, multi-walled carbon nanotube or alloys), are performed to quantify these biogenic amines [13–20]. When an unmodified electrode was used to carry out the anodic reaction, a thin layer of oxide (glassy carbon + films of nickel oxidized to nickel hydroxide Ni(OH)₂ and/or nickel oxyhydroxide NiOOH), appeared at the electrode surface, acting as catalyst for the electrooxidation of the amine; thus, the current integration during the cycle (oxidation followed by reduction) allows the charge involved for the oxide formation to be deduced. The charge involved for the indirect amine oxidation is deduced by the difference with the overall charge, and allows the amine percentage to be evaluated. Electrochemically modified electrodes could also be used to quantify the amines; they are obtained by electrodeposition, on glassy carbon

[a] D. Koita, C. Kane, M. Diaw, O. Sock
Laboratoire d'Electrochimie et des Procédés Membranaires,
Ecole Supérieure Polytechnique, Université Cheikh Anta
Diop de Dakar
BP:5085 Dakar-Fann, Sénégal

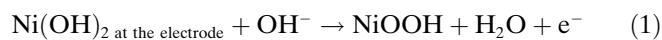
[b] T. Tzedakis
Laboratoire de Génie Chimique UMR CNRS 5503, Bât.
2RI, Université de Toulouse Paul Sabatier
118, Route de Narbonne, 31062 Toulouse Cedex 9, France
tel: +33(0)561558302
*e-mail: tzedakis@chimie.ups-tlse.fr

[c] P. Lavedan
Service Commun de RMN, FR2599, Université de Toulouse
Paul Sabatier
118, Route de Narbonne, 31062 Toulouse Cedex 9, France

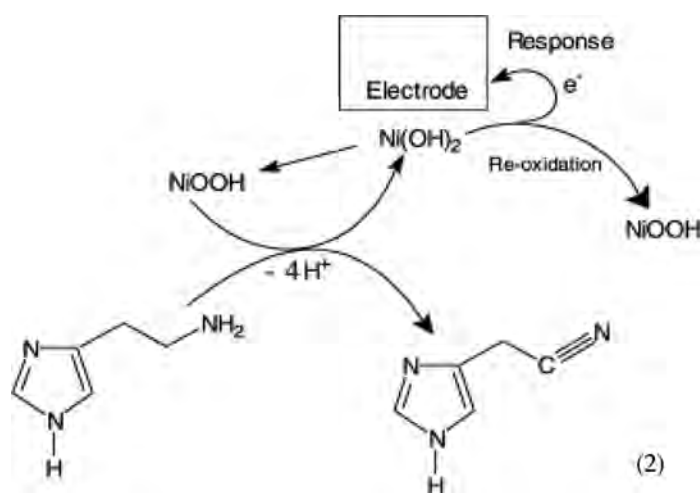
for example, of transition and/or precious metals, nickel powder for example.

Švarc-Gajić and al [19] propose the following reaction scheme for the indirect electrooxidation of the amine using solid nickel hydroxide as catalyst:

-Electro-oxidation of solid $\text{Ni}(\text{OH})_2$ to NiOOH ; indeed, authors claim that the $\text{Ni}(\text{OH})_2$ form a thin film on the anode which could be oxidized to soluble NiOOH , according to the Equation 1:



then soluble NiOOH chemically reacts with histamine and regenerates the $\text{Ni}(\text{OH})_2$ according to the schematic reaction mechanism (Equation 2).



Sensibility and reproducibility of results seems satisfactory and a short time was required to carry out this analysis.

Young et al. [25b] propose enzymatically assisted amperometric detection of histamine. The pyrroloquinone quinone co-enzyme was immobilized (entrapment) within a matrix of electroformed polypyrrole. The obtained sensor exhibits good sensitivity (mg/L of histamine) and satisfactory time life (>1 month). Detection of Histamine within a fish sample was achieved with success. Because various interferences with other compounds (mainly thiols, and some amines) even after using a nafion layer, authors suggest to use, after miniaturization, this device as detector for capillary electrophoresis systems.

Using the classical thin layer electrochemistry technique, this work aims to approach the histamine oxidation mechanism. Indirect oxidation of the histamine on platinum anodes was carried out in the presence of nickel sulfate, acting as a catalyst.

Thin layer electrochemical measurements, acting as macroelectrolysis of low volume samples, are very powerful for rigorously determining the exchanged electrons number of the overall process. Indeed, this is a macroelec-

trolysis of low volume samples and experimental curve integration provides the amount of charge enabling total conversion of the electroactive specie; determination of the electrode surface area, or other electrokinetic parameters does not required. So, the main preliminary objective is to understand the mechanism of the catalytic oxidation of histamine by nickel, since, to our knowledge, very few studies have been carried out [19]. As a function of the obtained results, a future objective of this study is to propose an analytical method, consisting of electrochemical measurements of histamine, simpler and more rapid than existing techniques. Solutions containing extracted histamine from fish will be analyzed in order to show that histamine can be detected and quantified by this method. The final objective is to propose a simple and rapid method which is able to provide an estimation of the histamine content from the solid food mixture, especially fish, by analysis of a thin layer of food paste.

2 Experimental

The chemicals used, potassium chloride, sodium hydroxide, Trichloroacetic acid, Histamine dihydrochloride, $\text{NiSO}_4 \cdot 6\text{H}_2\text{O}$, NaOH, were supplied by Acros, Sigma-Aldrich or Prolabo, and bi-distilled water was used for all solutions.

Potassium chloride (KCl 0.2 M) was used as supporting electrolyte, and NaOH was added to adjust pH to 12.6. Excess of the electrolyte ($C_{\text{electrolyte}} \sim >50$ fold $C_{\text{electroactive species}}$) enables migration flux of the electroactive species to be neglected, as well as the conductivity of the liquid film in the thin layer to be increased (partial compensation of the Ohmic drop).

All the measurements were carried out at room temperature ($19 < T$ ($^{\circ}\text{C}$) < 22). All solutions are 'room aerated solutions'; the presence of dissolved oxygen does not influence the anodic current of the involved system.

Electrochemical measurements were carried out using a Potentiostat-Galvanostat (PGZ 100-Voltalab of Radiometer Analytical and the VoltaMaster 4 software).

The electrochemical three-electrodes cell (Figure 1) was constituted of:

- i) a platinum grid as auxiliary electrode,
- ii) a saturated calomel electrode connected to a Luggin capillary, located near (3–4 mm) the working electrode (the inlet of the thin layer) and containing the electrolyte in large excess,
- iii) a platinum grid sandwiched between two glass microscope-slides, referred to as the thin layer.

Before manufacturing the thin layer, the platinum grid was burned until observation of a blue flame; this treatment enables the removal of all impurities from its surface; simultaneously platinum oxidizes and platinum oxide(s) appears on the metallic surface. Because the electrochemical response is strongly conditioned by the burning ([26–27]) we choose to burn the electrode, during fifteen minutes after the blue flame appears. Indeed, several types of oxides can appears such PtO , Pt_3O_4 , PtO_2

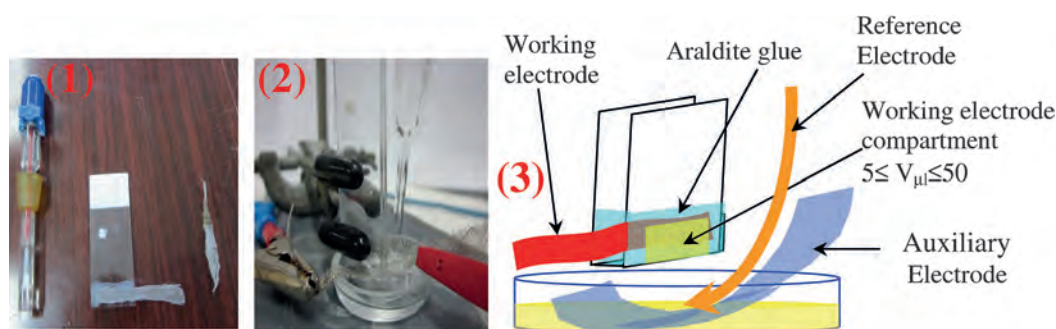


Fig. 1. 1) The three electrodes used to design the thin layer cell: saturated calomel electrode (left); thin layer with a platinum grid used as working electrode (middle); auxiliary electrode: platinum grid (right). 2) Picture of the electrochemical three electrodes cell used. 3) Schematic representation of the thin layer electrochemical cell.

[28–30] and reactivity of the electrode, (platinum successive oxidations, catalytic ability) can change.

Consequently, differences can occur in the electrochemically active area of platinum between the various thin layers used; nevertheless, in this study the electrochemical response attributed to the oxidation of the Ni/Histamine mixture (first signal) appears to be reproducible, while the massive signal, at higher potentials, undergoes effects of this phenomenon.

The thin layer was filled using a low volume (10 to 50 μL) syringe or Gilson micropipettes; for the suspension, only the supernatant solution (limpid/clear or not) was used to fill the electrolytic compartment. Figure 1 shows the electrochemical thin layer cell used.

A platinum grid (5 cm \times 0.8 cm) was sandwiched between two ‘microscope glass slides’ (2.5 cm \times 7.5 cm); a thin film of glue (around the platinum grid) allows defining the electrolytic compartment, whose volume and thickness (determined using a digital caliper) are respectively in the range of 10–50 μL and 100 to 500 μm as function of the thickness of the platinum grid (Figure 1,1).

Filling of thin layer was performed using micropipette; thus the volume of the analyzed solution could be determined precisely. The low potential scan rate, allows to operate in macroelectrolysis conditions and the whole electroactive species to be transformed. Note that in the thin layer electrochemistry and for simple electrochemical systems involving only an electron-exchange reaction, ‘peak-shaped’ curves are obtained and the magnitude of the peak current can be expressed as follows (Equations 3a and 3b), [31,32]:

$$I_{\text{peak}} = (n_{\text{over}}^2 F^2 r V_{\text{TL}} C) / (4RT) \quad (3a)$$

reversible system

and

$$I_{\text{peak}} = (n_{\text{over}} n_{\text{limstep}} F^2 r V_{\text{TL}} C) / (2.703RT) \quad (3b)$$

irreversible system

Note that, for more complicated systems (involving chemical reactions, associated with the electron exchange reaction) relations (Equations 3a and 3b) could not be applied. Nevertheless, here, as indicated above, the access to the exchanged electrons number was achieved by integrating the peak area to the experimental current potential curve.

The same thin layer can be used for various experiments, there is no ‘observed irreversible passivation’ of the platinum working electrode between the various experiments; indeed, reproducible curves were obtained for the Hm/Ni system oxidation (effect on the platinum signal does not examined) after rinsing the thin layer two-folds with water and one-fold with the fresh analyzed solution.

Histamine was extracted from the muscles of fish according to methods described in the bibliography [6,7]. After one day of exposing the fish to the sun (to increase the histamine content), 30 g of muscle were carved off various parts of the fish, and mixed with 90 cm^3 of trichloroacetic acid at 10%, in order to obtain a fine and uniform suspension.

After that, the suspension was filtered and the volume of the filtrate was reduced under vacuum (11 mm Hg); potassium chloride (0.2 M) was then added, the pH was adjusted to 12.6 and the final solution (47 cm^3) was kept at 4 $^\circ\text{C}$.

3 Results and Discussion

3.1 Study of the Electrochemical Behavior of the Various Reagents

Current potential curves obtained with the various reagents are indicated in Figure 2. Instead of the magnitude of the current, we chose to plot the ratio magnitude of the current/volume of the thin layer (see Equation 3) versus the electrode potential. The obtained signals were thus easier to compare.

Curve 1 is the residual current, obtained from a solution of KCl (0.2 M) at pH 12.6 without histamine nor nickel; it shows a nicely resolute peak starting around 0.55 V for

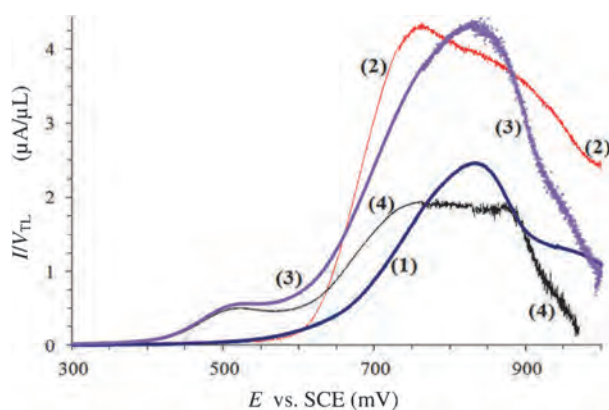
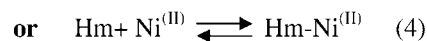
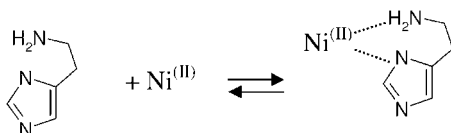


Fig. 2. Current potential curves obtained by thin layer electrochemistry, on platinum anode, with the various reagents involved in this study. KCl (0.2 M); $r=0.3$ mV/s; pH 12.6. 1) Residual current (blank). Same curve as (1) obtained in presence of Hm (10^{-3} M). 2) Solution of curve (1) without Hm + $\text{NiSO}_4 \cdot 6\text{H}_2\text{O}$ (10^{-3} M). 3) Solution of curve (2) + Hm (10^{-3} M). 4) Curve resulting after subtraction of curve (1) from curve (3).



which the max current was located at ~ 0.82 V, attributed to the platinum/platinum oxide electrode to higher platinum valences (Pt_xO_y) [28–30].

Addition of histamine (10^{-3} M) to the solution does not modify the shape of the signal (obtained curve – not represented here is the same as (1)) but the magnitude of the current slightly ($\sim 5\%$) less (the second scan indicates the same curve, there is no cumulative drop in the current), probably caused by a partial passivation of the anode due to histamine adsorption. Another reason could be a slight decrease in solution conductivity; this introduces an additional ohmic drop (at constant applied voltage) that led to the slight drop of the current.

Curve 2 was obtained when $\text{NiSO}_4 \cdot 6\text{H}_2\text{O}$ (10^{-3} M) was added to the KCl (0.2 M)/pH 12.6 solution. Note that the resulting mixture was a suspension, at pH 12.6. The stable form of $\text{Ni}^{(\text{II})}$ is the $\text{Ni}(\text{OH})_2$, concentration of Ni^{2+} was extremely low ($(10^{-14.7}/(10^{-1.4})^2) \approx 10^{-12}$ M). The curve indicates the presence of a peak, commencing approx. 0.6 V for which the maximum current was located at ~ 0.75 V, followed by a shoulder (0.8–1 V). Signals were attributed respectively to the oxidation of $\text{Ni}^{(\text{II})}$ to $\text{Ni}^{(\text{III})}$ and to the platinum/platinum oxide electrode to higher platinum valences (Pt_xO_y) [28–30].

The presence of solid particles of $\text{Ni}(\text{OH})_2$ and/or NiOOH could explain a certain irreproducibility of current magnitude of this overall signal.

Curve 3 corresponds to the oxidation of a mixture containing KCl (0.2 M), $\text{NiSO}_4 \cdot 6\text{H}_2\text{O}$ (10^{-3} M) and Histamine (10^{-3} M). The mixture contains a ‘slight’ fraction of

solid particles of the nickel sulfate, (26 mg of the powder was dissolved in 100 cm^3 ; it remains less than 5 solid particles of a diameter less than 0.5 mm) a significant quantity of the solid $\text{Ni}^{(\text{II})}$ appears to be dissolved in presence of histamine; nevertheless, as a function of Hm content, the obtained solution was not perfectly limpid/clear, due to the presence of fine non-dissolved particles of nickel hydroxide or hydrates (this point was not investigated). A ‘low magnitude’ new signal appears in the potential range from 0.4 to 0.6 V, followed by the global signal (0.6/1 V) previously observed in curve 2.

As observed in curves (1) and (2), the first signal (0.4 to 0.6 V) was not present with nickel or histamine alone; it arises from the oxidation of an adduct resulting from complexation of Hm with $\text{Ni}(\text{OH})_2$, according to the following expected equilibrium (4). The resulting $\text{Hm-Ni}^{(\text{II})}$ complex appears to be ‘stable’ because dissolution of the $\text{Ni}(\text{OH})_2$ takes place and shifts the equilibrium (Equation 4) to the forward direction.

Nickel/histamine complexes, such as $\text{Ni}(\text{Hm})\text{Cl}_2$ and $[\text{Ni}(\text{Hm})_3]\text{Cl}_2$, have been investigated in the far-infrared region by Drozdowski et al. [33]. Metal isotope labelling and deuteration effects were employed for observed band assignments. Metal-ligand vibrations were discussed and correlated with the structures of these complexes (of which the geometry appears to be similar with that suggested in Reaction 4).

Altun et al. [34] carry out various potentiometric studies and concludes in the existence of binary and mixed-ligand complexes, formed with histamine and some transition metals ($\text{Cu}^{(\text{II})}$, $\text{Ni}^{(\text{II})}$, $\text{Zn}^{(\text{II})}$, ...). Authors propose complexation constants for the various aqueous equilibria; they discuss on the ability of the amino group to acts as the primary anchor site for metal ions and, as such, to promote the stepwise deprotonation and subsequent coordination of other successive binding sites, leading to the formation of the hydrolytically stable, fused, five-membered chelate rings with M–N bonds.

Moreover several other works [35,36] centered on biological applications carried out to study complexation of histamine and others ligands with $\text{Ni}^{(\text{II})}$. Young et al. [35] demonstrates the inhibition of histamine in the brain by complexation with $\text{Ni}^{(\text{II})}$. Reddy et al. [36] investigate the complexation of $\text{Ni}^{(\text{II})}$ ethylene diamine with histamine as well as their DNA cleavage abilities; authors use various techniques (such as ESI-MS analysis) to demonstrates i) the existence, ii) the geometry, ii) the concentration distribution of ternary complexes $\text{Ni}/\text{Hm}/\text{ethylene diamine}$, and finally iv) to determine the stability constants of these complexes.

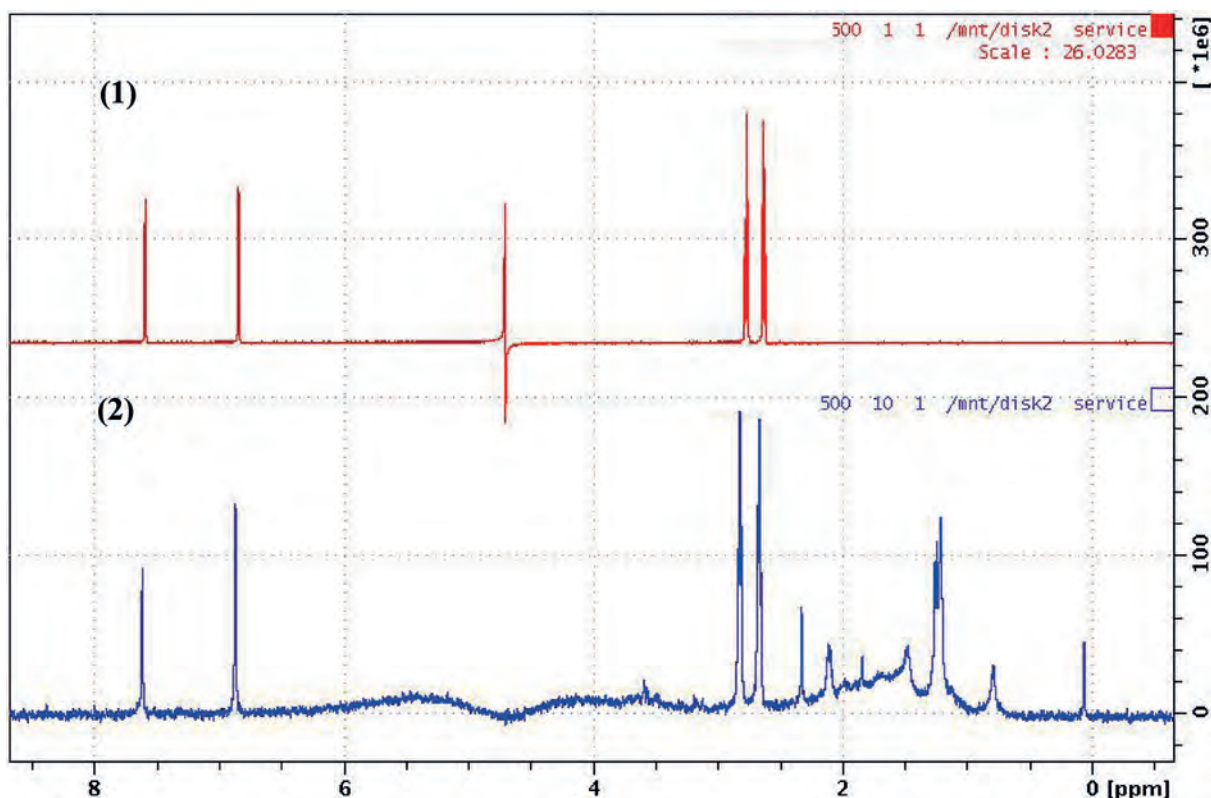


Fig. 3. NMR spectra obtained at 298 K on a Bruker AVANCE 500 MHz spectrometer equipped with a 5 mm Z-gradient TBI probe. The 90° pulse length: $10.5 \mu\text{s}$; sweep width: 10 kHz; acquisition time: 3.5 s. The scan number was adjusted to obtain a sufficient signal to noise ratio. 1) red line, ^1H NMR of histamine in D_2O with water suppression (zgpr pulseprogram of the Bruker library). 2) blue line, ^1H NMR of histamine with NiSO_4 in D_2O and H_2O . The acquisition was achieved fourteen hours after the mixing with water suppression using watergate to optimize sensitivity (zgpgw5 pulseprogram of the Bruker library).

Various experiments were achieved to demonstrate the existence of the equilibrium (Equation 4) in the present experimental conditions:

i) two sets of $\text{Ni}^{(\text{II})}/\text{Hm}$ mixtures, containing KCl at pH 12.6, were prepared in order to observe the physical state of the suspension (presence or not of solid particles).

i-a) a first series of suspensions was prepared: suspensions contain a constant concentration (10^{-3} M) of histamine, and concentrations of $\text{Ni}^{(\text{II})}$ varying in the range from 0.1×10^{-3} to 10^{-3} M.

All mixtures containing $\text{Ni}^{(\text{II})}$ at concentrations higher than 5×10^{-4} M, indicates the presence of solid $\text{Ni}^{(\text{II})}$. A perfectly clear solution was obtained for concentrations of $\text{Ni}^{(\text{II})}$ equal or lower than 10^{-4} M, the whole $\text{Ni}^{(\text{II})}$ solid particles dissolve in these kinds.

i-b) a second series of various suspensions was prepared: suspensions contain a constant concentration (10^{-3} M) of $\text{Ni}^{(\text{II})}$, and concentrations of histamine varying in the range from 10^{-3} to 7×10^{-3} M. Observed precipitate ($\text{Ni}(\text{OH})_2$) in the mixture, disappears for Hm concentrations higher than 3×10^{-3} M. Dissolution of solid nickel hydroxide confirms the existence (in the current operating conditions) of the chemical equilibrium between both species ($\text{Hm}/\text{Ni}^{(\text{II})}$).

ii) Additional experiments were achieved by NMR in order to confirm the formation of the $\text{Hm-Ni}^{(\text{II})}$ complex. Figure 3 presents ^1H NMR spectra obtained at 298K with various mixtures.

Spectrum (1), a red line, corresponds to a histamine solution. Signals at 2.6 and 2.8 ppm were attributed to the $-\text{CH}_2-$ of the primary amine group. Signals at 6.8 and 7.6 ppm were attributed to the H located in alpha position of the H-N group of the ring.

Low sensitivity for nickel of the Bruker AVANCE 500 MHz spectrometer, prevents obtaining spectra containing a signal. Spectrum (2), a blue line, corresponds to a mixture containing NiSO_4 and histamine (in excess) in D_2O and H_2O . The histamine excess with respect to the nickel causes the presence of signals in spectrum (1).

In addition, the spectrum presents several signals in the range from 1 to 2.5 ppm. These signals were attributed to one $\text{Hm-Ni}^{(\text{II})}$ complex (at the least, because several chelates could co-exists in solution as showed in various studies [33–36]); a donor-acceptor bond between the Ni and the N of the primary amine group shield the H of the $-\text{CH}_2-$ group and causes the observed chemical shift of signals.

iii) The nature of the signal at 0.4 to 0.6 V (curve 3, Figure 2) will be elucidated in the next session; let us

note that the reverse scan (curve 3, Figure 2), does not show the presence of cathodic signals in the potential range of 1 to -0.2 V (the obtained curve overlays with the X-axis), demonstrating an irreversible behavior of the system Hm-Ni^(II)/(Hm-Ni^(III)).

Subtraction of the curve (1) Figure 2, from the curve (3), gives the curve (4), which clearly shows the Hm-Ni^(II) oxidation 'peak', as well as a low resolution signal, attributed to the oxidation of the residual 'un-complexed' Ni^(II) fraction, mainly present as fine (Ni(OH)₂) precipitate.

3.2 Ni^(II) Concentration Influence on the Anodic Response of the System (Hm/Ni^(II))

The effect of the NiSO₄ concentration (in presence of histamine) on the curves $I=f(E)$ was examined in order to try to understand the first signal of the curve 3 Figure 2. It is expected that it confirms the existence of the Ni^(II)/Hm equilibrium; moreover it could allow estimation of some data in relation with this equilibrium. Curve (1) Figure 4 confirms oxidation of both platinum and Ni^(II), as shown previously (Figure 2, curve (2)). Curves 2, 3 and 4, obtained for [Hm]/[Ni(II)] ratios in the range of 10 to 1, present the signal (0.4 to 0.6 V) previously attributed to the oxidation of the Hm-Ni^(II) complex.

For [Hm]/[Ni^(II)]=1 mM/0.1 mM=10, the mixture obtained was totally limpid, absent of precipitates. All Ni^(II) was complexes with histamine (4).

Curve (2), obtained for this ratio, contains two signals satisfactorily resolute at 0.4–0.6 V and 0.6–0.9 V. The first is attributed to complex Hm-Ni^(II) oxidation arising from complete dissolution and complexation of Ni^(II) by excess Hm; the second corresponds to the Pt electrode oxidation. There is no free Ni^(II) in the solution, so the shoulder in the potential range 0.85 to 0.95 V is absent; note that

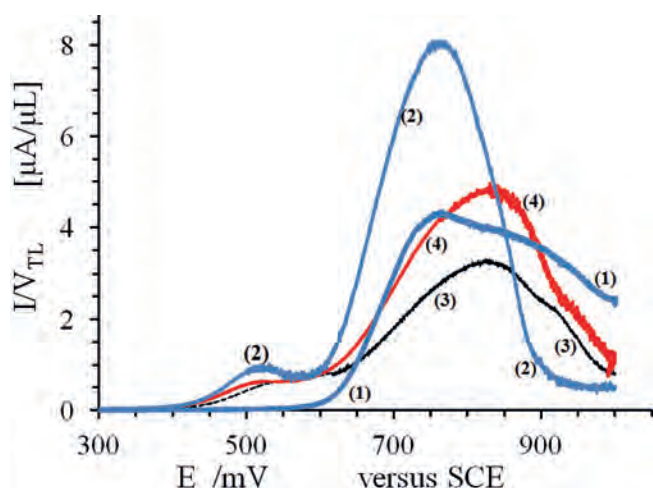


Fig. 4. Nickel sulfate concentration dependence of the current-potential curve shapes, obtained by thin layer electrochemistry on Pt anode. KCl (0.2 M); $r=0.3$ mV/s; pH 12.6. 1) NiSO₄·6H₂O (1 mM); 2), 3) and 4) Hm (1mM)+ NiSO₄·6H₂O at respectively 0.1 mM, 0.5 mM and 1 mM.

for higher concentrations of NiSO₄·6H₂O (1 mM) e.g. curve 4 Figure 4, this shoulder is present and its magnitude decreases.

The current magnitude of the second signal (curve 2, Figure 4), is important in comparison to the shoulder of the curve (1), expected to correspond to free Ni^(II) and Pt simultaneous oxidation. Differences in current magnitudes indicates Pt oxidation was affected by solid Ni^(II) which could deposit and modify the state of the area of the platinum grid.

Moreover, comparison of signal magnitudes at approximately 750 mV (expected values corresponding to the platinum oxidation) for curve 1 Figure 2 and curve 2 Figure 4, reveals important differences, probably arising from burning the platinum grid.

A rough estimate of the equilibrium constant of reaction 4 was carried out for the following conditions:

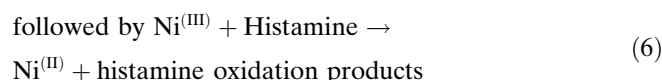
	Hm	Ni ^(II)	Hm – Ni ^(II)
<i>Initial</i>	1mM	0.1mM	–
<i>Equilibrium</i>	0.9mM	(10 ^{-14.7}) ^{0.5} M	0.1mM

Indeed, the ratio [Hm]/[Ni^(II)]=10 leads to a totally clear mixture, without precipitates.

The value obtained ($K_4=2.5 \times 10^6$) seems relatively high; nevertheless, it seems to be in agreement with an apparent equilibrium constant for the Hm-Ni^(II) formation, estimated using the peak potential lowering of 0.4 V e.g. difference from ~ 0.9 V (oxidation of 'free' Ni^(II)) until ~ 0.5 V (oxidation of the nickel-Hm complex) which leads to a value of $\exp(1 \times F \times 0.4 / RT) = 5 \times 10^6$.

For higher Ni^(II) concentrations and [Hm]/[Ni^(II)] ratios from 2 to 1, the mixture obtained contains a slight suspension (presence of Ni(OH)₂), and curves (3) and (4) of Figure 4, indicate the presence of the three expected anodic signals; their current magnitudes do not significantly change with the Ni^(II) concentration. We note a very slight decrease in signal current magnitude at 0.4–0.6 V, as well as a shift to the more anodic potentials of the second 'massif', probably caused by the Ni(OH)₂ precipitates to the platinum grid.

Švarc-Gajić et al. [19] have studied the oxidation of Ni^(II) in the presence of histamine on vitreous carbon, modified by nickel, in presence of NaOH. Author attribute the observed signal at 0.36 V to the oxidation of Ni(OH)₂ to NiOOH (Equation 5), followed by a Chemical Reaction 6 between NiOOH and histamine, which allows Ni(OH)₂ to regenerate:



Our study concludes that histamine complexes Ni^(II) according to reaction (4) and especially before the electro-

chemical reaction; the resulting adduct Hm-Ni^(II) is electroactive (Equation 7) for potentials higher than 0.4 V/SCE, where Ni^(II+x)-HmP is the electrogenerated Ni/histamine oxidation product.



Note that under the same conditions, oxidation of ‘free’ Ni^(II) is more difficult than oxidation of nickel complexes, which takes place for higher potentials (0.6/0.7 V/SCE). Determination of the exchanged electron numbers will be studied in the next paragraph.

3.3 Histamine Hm Concentration Influence on the Anodic Signals of the System (Hm/Ni^(II))

In order to provide additional proof regarding the existence of the complexation between Ni^(II) and Histamine (e.g. Reaction 4), as well as the corresponding equilibrium, current potential curves were plotted by keeping constant the Ni^(II) concentration (1 mM) and by varying the histamine concentration in the range (1 to 7 mM). Curves obtained (Figure 5), show that the low resolution signal, previously attributed to the oxidation of Ni^(II)-Histamine complex (Figure 4 curve 2) appears as a clear peak when histamine concentration increases. In addition the peak shifts to the lower potentials meaning a certain stabilization of the generated complex by an excess of histamine.

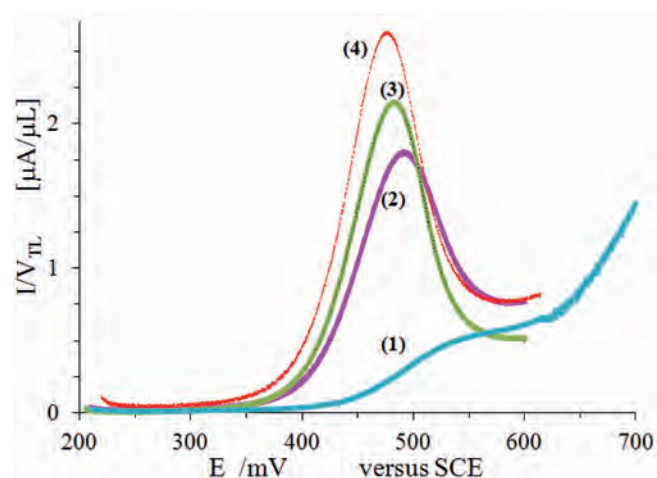
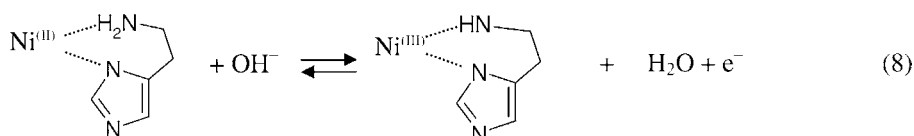


Fig. 5. Histamine concentration dependence of the current-potential curve shapes, obtained by thin layer electrochemistry on Pt anode. KCl (0.2 M); $r=0.3$ mV/s; pH 12.6; NiSO₄·6H₂O (1 mM). (1) to (4): Hm at 10⁻³ M, 3×10⁻³ M, 5×10⁻³ M and 7×10⁻³ M respectively.



Note that increasing the histamine concentration causes the disappearance of the shoulder present in the potential range from 0.85 to 1 V of the $I=f(E)$ curves (Figure 5), the peak of platinum oxidation was only observed.

These results confirm the whole dissolution of solid Ni^(II) according to the Reaction 4.

Figure 6 (extracted from Figure 5) indicates the influence of histamine concentration on the ratio magnitude: peak current/thin layer volume. A linear evolution was observed for concentrations less than 3 mM, while curve asymptotically tends to an I_p/V_{TL} value of 2.6 μA/μL.

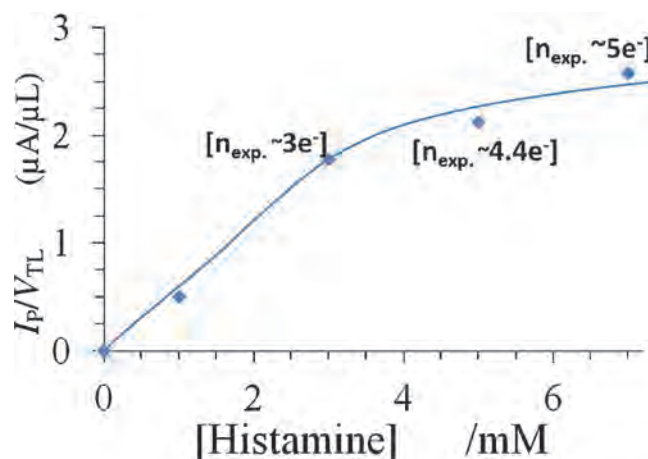
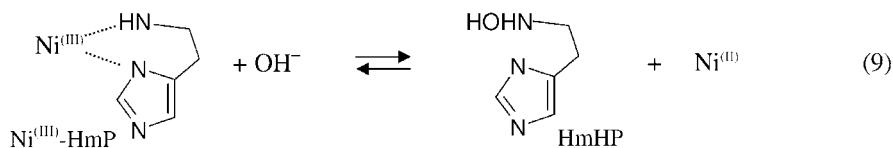


Fig. 6. Histamine concentration dependence on magnitude (expressed as $I_{\text{peak}}/V_{\text{TL}}$) of the Hm-Ni^(II) oxidation signal. Results extracted from Figure 5.

Moreover, the graphical integration of the peak (0.35–0.6 V) in the experimental curves of Figure 5, provides the amount of charges required for the total conversion of the electroactive species into the thin layer, and allows access to the exchanged electrons number during oxidation (and indicated in Figure 6): 3, 4.4 and 5 for concentrations of histamine 3, 5 et 7 mM respectively, the initial Ni^(II) concentration was maintained at 1 mM.

The results clearly indicate that the determined electron number does not correspond to the oxidation of the Ni^(II) alone; indeed, in this case, the expected electron number must be 1, for all the histamine concentrations examined. On the other hand the electron number was lower than this expected for a total conversion of histamine, involving 1 electron/mol (especially for histamine concentrations higher than 3 mM).



To explain the obtained electron numbers, we propose the following remarks and comments:

a/-The resulting complex is electroactive and it can be undergoing an ‘one-electron’ oxidation, according to reaction (7) or (8) where $x = 1$.

Indeed, for concentrations of $\text{Ni}^{(\text{II})} = 1 \text{ mM}$ and concentrations of histamine in the range 1 to 3 mM, the electron number obtained corresponds to ‘one electron exchanged per mole of Hm’; this implies that $\text{Ni}(\text{II})$ complexes Hm and resulting adducts can be oxidized according to the reaction (7); the electrogenerated product ($\text{Ni}^{(\text{II}+x)\text{-HmP}}$) is $\text{Ni}^{(\text{III})}\text{-HmP}$ and in presence of NaOH, this adduct decomposes according to the reaction (9), to provide histamine hydroxylated product (HmHP), and simultaneously $\text{Ni}^{(\text{III})}$ is reduced to $\text{Ni}^{(\text{II})}$, which immediately seize a new histamine molecule, and achieves a new ‘catalytic-cycle’. This sequence is repeated until complete indirect oxidation of Hm, providing HmHP and $\text{Ni}^{(\text{II})}$ free in the solution (probably under solid form, because the interruption of the polarization at 600 mV, see Figure 5).

Then, the $\text{Ni}^{(\text{III})}\text{-Hm}$ is involved in a new oxidation/decomposition cycle, and this electrocatalytic scheme continues practically until total oxidation of histamine, that could explain the observed electron number.

b/-Let us note that for higher concentrations of histamine (5 mM to 7 mM), we can assume that the majority of the $\text{Ni}^{(\text{II})}$ was complexed and present under $\text{Ni}^{(\text{II})}\text{-Hm}$ form. In this type of situation, the expected electron number has to be 5, and 7 for the examined concentrations. However, experience does not confirm this; the obtained electron numbers are respectively 4.4 and 5. We suggest two explanations:

b-1/ for all experiments $\text{Ni}^{(\text{II})}$ initial concentration is the same (1 mM), but the histamine concentration varies with the ratio $[\text{Hm}]/[\text{Ni}^{(\text{II})}] = 1$ to 7. Assuming that the chemical reaction (9), following the electrochemical one [(7 or 8) here $x = 1$] is rapid, we can conclude that during the scan of the potentials, the Hm concentration decreases; when this concentration becomes lower than the $\text{Ni}^{(\text{II})}$ initial concentration (1 mM), part of the $\text{Ni}^{(\text{II})}$ could precipitate ($\text{Ni}(\text{OH})_2$), and this quantity will increase with histamine concentration decrease. The consequence is that the histamine conversion cannot be complete, because equilibrium (4) cannot be reached.

b-2/ On the contrary, the chemical reaction (9) would be slower than the electrochemical one (8); in this kind of situation, the complex $\text{Ni}^{(\text{III})}\text{-HmP}$ produced at the electrode can cumulate and the available $\text{Ni}^{(\text{II})}$ concentration (makes it possible to reach equilibrium (Equation 4)), decreases during the current potential plot. Obtained current, charge and consequently electron number

were lower than expected. Let us note that both effects (solid $\text{Ni}(\text{OH})_2$ and accumulated $\text{Ni}^{(\text{III})}\text{-HmP}$) could act simultaneously and affect the experimentally determined electron number.

3.4 Potential Scan Rate Influence on the Electrochemical Behavior of the System $\text{Ni}^{(\text{II})}/\text{Hm}$

The influence of the potential scan rate on the anodic peak (0.3–0.5 V) attributed to the oxidation of the complex $\text{Ni}^{(\text{II})}\text{-Hm}$, was examined and results (Figure 7) give rise to the following comments and remarks:

-Increasing the potential scan rate shifts the peak towards the anodic potentials. A linear evolution of the peak potential versus the logarithm of the product “electrode surface area/thin layer volume/potential scan rate” was observed (Figure 8 (a)), showing the irreversible behavior of the system.

$$\begin{aligned} E_{\text{peak}} &= E^{\circ'} - (RT/(an_{\text{lim step}}F)) \\ &\times (\ln(RTk^{\circ}/(an_{\text{lim step}}F)) + \ln(S/(rV_{\text{TL}}))) \\ &= 0.6 - 0.02 \times \ln(S/(rV_{\text{TL}})) \\ R^2 &= 0.98 \end{aligned} \quad (10)$$

Slope of the obtained linear correlation (10) led to the anodic electronic transfer coefficient $an = 0.9$, a relatively

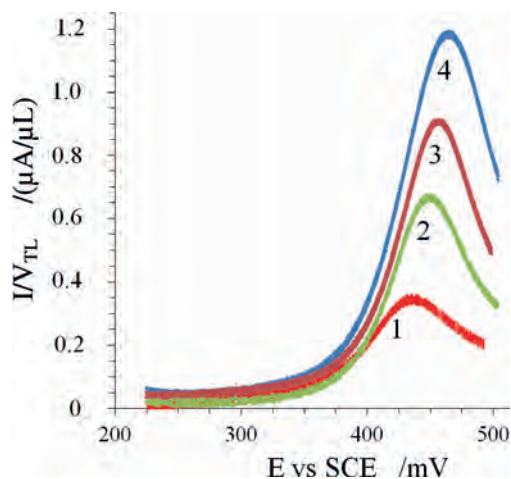


Fig. 7. Potential scan rate dependence of the magnitude of the Hm- $\text{Ni}^{(\text{II})}$ oxidation signal. $I = f(E)$ curves obtained by thin layer electrochemistry on Pt anode. KCl (0.2 M); pH 12.6; $\text{NiSO}_4 \cdot 6\text{H}_2\text{O}$ (1 mM); Hm (5 mM). (1) $r = 3.6 \text{ mV min}^{-1}$, $V_{\text{TL}} = 12 \text{ } \mu\text{L}$; (2) $r = 6 \text{ mV min}^{-1}$, $V_{\text{TL}} = 22 \text{ } \mu\text{L}$; (3) $r = 9 \text{ mV min}^{-1}$, $V_{\text{TL}} = 25 \text{ } \mu\text{L}$; (4) $r = 12 \text{ mV min}^{-1}$, $V_{\text{TL}} = 25 \text{ } \mu\text{L}$.

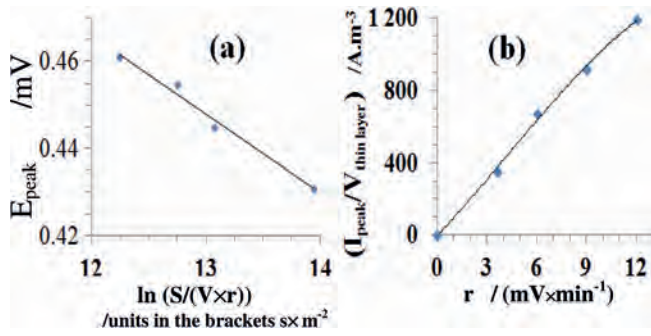


Fig. 8. Results extracted from Figure 7. a) Peak potential dependency versus $\ln(S/(Vr))$; b) Potential scan rate dependency on the ratio $I_{\text{peak}}/V_{\text{TL}}$.

high value for an irreversible system, taking account 1 electron exchanged in the rate determining step.

Irreversibility was also confirmed by the absence of cathodic signals during the reverse scan in the potentials range of 0.5 to -0.2 V (curves not represented).

Results' analysis (Figure 7) led to a non linear evolution (as required for a simple system in the thin layer electrochemistry) of the ratio $I_{\text{peak}}/V_{\text{TL}}$ against the potential scan rate (Figure 8b), even if the operating values of r remain low (< 12 mV/min).

Chosen concentrations of Hm (5 mM) and $\text{Ni}^{(\text{II})}$ (1 mM) enable equilibrium (Reaction 4) to be reached before plotting curves, so the expected initial concentration of the $\text{Ni}^{(\text{II})}$ -Hm complex remains constant but does not explain the curve obtained. The absence of linearity could be caused by the chemical Reaction 9 following the electrochemical one (8). Indeed, increasing the potential scan rate causes the current to increase, producing higher quantities of adduct $\text{Ni}^{(\text{III})}$ -HmP, which can cumulate. Consequently the available concentration of $\text{Ni}^{(\text{II})}$ -Hm decreases and the current magnitude obtained is lower than the expected one.

Finally, the simplified reaction scheme indicated in Figure 9 could be put forward:

Mass balance for $\text{Ni}^{(\text{III})}$ -HmP within the thin layer could be written as follows:

$$\begin{aligned}
 0 &= \text{chemical Reaction 9 flux} \\
 &- \text{electrochemical Reaction 8 flux} + \text{accumulation flux} \rightarrow \\
 0 &= r_{(9)} \times V_{\text{TL}} - I / (n_{\text{over}} \times F) + V_{\text{TL}} \times dC/dt
 \end{aligned}
 \tag{11}$$

Where:

- * $r_{(9)}$ = rate of the chemical Reaction 9, assumed to obey to a II^{d} order = $k' \times [\text{Ni}^{(\text{III})}\text{-HmP}] \times [\text{OH}^-]$;
- * C° = the initial concentration of $\text{Ni}^{(\text{II})}$ = $[\text{Ni}^{(\text{III})}\text{-HmP}] + [\text{Ni}^{(\text{II})}\text{-Hm}] + [\text{Ni}^{2+}] = C + C' + C'' \sim C + C'$
- * C'' , the $[\text{Ni}^{2+}]$, was assumed to be negligible;
- * because NaOH is in excess (0.044 M), $r_{(9)} = k \times C$, where $k = k' \times [\text{OH}^-]$

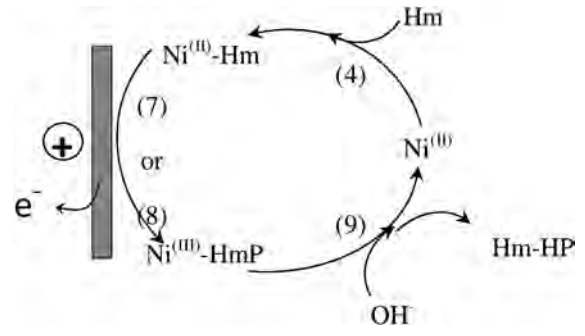


Fig. 9. Simplified reaction scheme proposed for the catalytic oxidation of Hm by NiSO_4 in alkaline media.

The current of the electrochemical reaction can be expressed by:

$$\begin{aligned}
 I &= (n_{\text{over}} F S C' k^\circ \times \exp((a n_{\text{lim step}} F / (RT))) \\
 &\times (E_{I=0} - E^{o'} + rt))
 \end{aligned}
 \tag{12}$$

Mass balance (Equation 11) can be explicit:

$$\begin{aligned}
 dC/dt &= (Sk^\circ / V_{\text{TL}}) \times (C^\circ - C) \\
 &\times \exp((a n_{\text{lim step}} F / (RT))) \times (E_{I=0} - E^{o'} + rt) - k C
 \end{aligned}
 \tag{13}$$

Solution of the Equation 13 permits accessing the temporal concentration profile for an arbitrary value of the apparent rate constant k of the Chemical Reaction 9; then, the substitution of this concentration in Equation 12 allows access to the current, and to compare its value to the experimental one (Figure 7). The good agreement between the two concentrations profiles allows determination of the constant, apparent rate k of the Chemical Reaction 9).

Another possibility consists in choosing constant values for the term $I/(n_{\text{over}} \times F)$ in the Relation 11, for the various potential scan rates; integration of this equation in this simplified case and from t_1/C_1 to t_2/C_2 , led to:

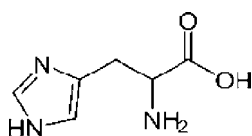
$$\begin{aligned}
 k &= (I/V_{\text{TL}} - I \times k \times \exp(t_2 - t_1)) / V_{\text{TL}} / \{n_{\text{over}} F (C_2 - C_1 \times k \\
 &\times [\exp(t_2 - t_1)])\}
 \end{aligned}
 \tag{14}$$

Each value of the term $I/(n_{\text{over}} \times F \times V_{\text{TL}})$ gives a set of times for the various potential scan rates (Figure 7), and consequently a set of concentrations C of the $\text{Ni}^{(\text{III})}$ -HmP adduct. A combination of these concentrations allows, using relation (14), the order magnitude of the apparent rate constant k of the Chemical Reaction 9: $(2 \pm 1) \times 10^{-6}$ to be estimated. Taking into account the NaOH excess (0.044 M), k' was estimated to be a relatively low rate constant $4.5 \times 10^{-8} \text{ m}^3 \text{ mol}^{-1} \text{ s}^{-1}$.

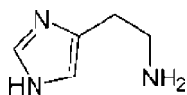
4 Histamine Content in the Fish Determination

Since the presence of histamine in food can cause intoxication, its content in commercialized fish and fish products has to be lower than 0.2 g/kg of fish [2].

Firstly, *Pagellus Bellottii*, fish from Senegal were used. This type of fish contains a high content of histidin (Scheme a) an amino-acide, which can be transformed into histamine (Scheme b) by selective action of bacteria like *Morganella morgani*, *Klebsiella* and *Hafnia* [37–38]. After exposure to the sun ($30 < T (^{\circ}\text{C}) < 45$ for 2 days),



Scheme a. Histidine



Scheme b. Histamine.

a sample of this fish was prepared according to the histamine extraction process described in § II.2. The extraction mixture obtained was analyzed by plotting the potential-current curves, and results are indicated in Figure 10 curve (8). Curve (8) indicates three signals respectively at 0.34, 0.72 V and for potentials higher than 0.9 V. Comparison of the potential of the first peak (0.34 V) with the corresponding one of the Ni^{II} -Hm complex (0.51 V, curve 1 Figure 10) shows an important difference (0.17 V), which cannot be attributed to the Ni^{II} -Hm complex oxidation. According to the same analysis, the second peak located at 0.72 V (curve 8) is also located far from this one of the histamine complex.

To try to explain what happens and to attribute these signals, an additional systematic study was performed and results are presented in Figure 10.

Curve 2 was plotted using solution containing histamine (commercial product) at higher concentrations (10 mM and $\text{NiSO}_4 \cdot 6\text{H}_2\text{O}$ 1 mM). The peak of histaminic complex was present at practically the same potential, and its current magnitude increases twice. A second peak was observed at potentials higher than 900 mV; it is attributed to the platinum oxidation, shifted to the anodic values, probably because histamine, present at high concentra-

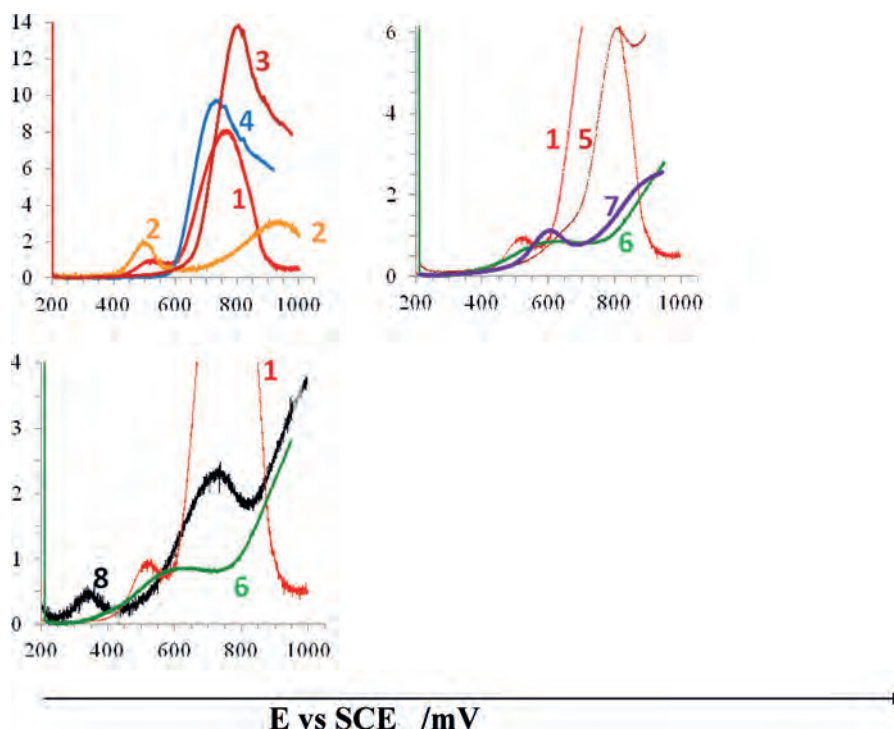


Fig. 10. Potential current curves obtained by thin layer electrochemistry on platinum anode. KCl (0.2 M); $r=0.3$ mV/s; pH 12.6. 1) Hm commercial product (5 mM) + $\text{NiSO}_4 \cdot 6\text{H}_2\text{O}$ (0.1 mM); 2) Hm commercial product (10 mM) + $\text{NiSO}_4 \cdot 6\text{H}_2\text{O}$ (1 mM). 3) 5 g of fish mixed in 20 mL of HClO_4 ; liquid fraction was analyzed after natural decantation; 4) (3) + $\text{NiSO}_4 \cdot 6\text{H}_2\text{O}$ (1 mM); liquid fraction was analyzed after natural decantation; 5) (3) + Hm commercial product (50 mM) + $\text{NiSO}_4 \cdot 6\text{H}_2\text{O}$ (1 mM); liquid fraction was analyzed after natural decantation; 6) 5 g of fish mixed in 20 mL of HClO_4 in presence of Hm commercial product (50 mM) and $\text{NiSO}_4 \cdot 6\text{H}_2\text{O}$ (20 mM). The resulting mixture was centrifuged, the solid was removed, then liquid fraction was analyzed. 7) 5 g of fish mixed in 20 mL of HClO_4 in presence of Hm commercial product (70 mM) and $\text{NiSO}_4 \cdot 6\text{H}_2\text{O}$ (10 mM). The resulting mixture is centrifuged and decanted. Liquid fraction was analyzed. 8) 30 g of a fish, exposed for two days to the sun, was mixed in HClO_4 in presence of $\text{NiSO}_4 \cdot 6\text{H}_2\text{O}$ (0.1 mM). The resulting mixture was centrifuged and the solid was removed. The resulting oily and viscous liquid fraction (47 cm^3) was analyzed.

tions adsorbs on the anode and passives this electrode. This adsorption is also responsible for the decrease in magnitude of the platinum oxidation peak. Fresh fish, not containing histamine, was mixed with HClO_4 and the suspension obtained ($S_{\text{mix/fish}}$) was analyzed. The obtained curve 3 (Figure 10) with a part of the decanted solution indicates the platinum oxidation peak ($E_{\text{peak}} \sim 795 \text{ mV}$), without any passivation.

$\text{NiSO}_4 \cdot 6\text{H}_2\text{O}$ (1 mM) was added to the previous suspension ($S_{\text{mix/fish}}$) and the I/E curve (4, Figure 10) obtained with this decanted solution, shows a peak centered at a slightly lower potential ($E_{\text{peak}} \sim 749 \text{ mV}$) than the previous one. Absence of $\text{Ni}^{(\text{II})}$ -Hm complex signal confirms the absence of Histamine ($< 10 \text{ mg/kg}$ of fish) in the fresh fish. The observed signal was attributed both to the oxidation of the dissolved $\text{Ni}^{(\text{II})}$ as well as the oxidation of platinum; the lower current observed is probably due to a slight passivation of the anode by the solid nickel sulfate, partially present in the mixture; the nickel peroxide was formed by $\text{Ni}^{(\text{II})}$ oxidation.

Histamine commercial product (50 mM) and $\text{NiSO}_4 \cdot 6\text{H}_2\text{O}$ (1 mM) were added to the suspension ($S_{\text{mix/fish}}$) and the I/E curve (5, Figure 10) obtained with the decanted solution shows a shoulder (from 500 to 660 mV), followed by a low resolution peak centered at $E_{\text{peak}} \sim 805 \text{ mV}$. The shoulder is attributed to the oxidation of $\text{Ni}^{(\text{II})}$ -Hm complex indicating $\text{Ni}^{(\text{II})}$ by Hm complexation, because of the high concentration ratio ($[\text{Hm}]/[\text{Ni}^{(\text{II})}] = 50$). Increase of its potential and low resolution of this signal can be explained by the adsorption of Hm to the electrode and the resulting passivation. Presence of other amines in solid fragments of the sample of the fish mixed could also complex the $\text{Ni}^{(\text{II})}$ and cause a slight decrease in the magnitude of this signal. This passivation was also responsible for the increase in peak potential (0.81 V instead 0.74 V) of platinum oxidation, as well as its low resolution.

Histamine commercial product (50 mM) and $\text{NiSO}_4 \cdot 6\text{H}_2\text{O}$ (20 mM) were added to the suspension ($S_{\text{mix/fish}}$) and the resulting mixture was centrifuged, the solid removed, then the liquid fraction was analyzed. The obtained I/E curve (6, Figure 10), shows a low resolution peak (from 400 to 750 mV), followed by an exponential part starting at $\sim 750 \text{ mV}$.

High concentrations of nickel sulfate added ($[\text{Hm}]/[\text{Ni}^{(\text{II})}] = 2.5$), leads to equilibrium (4) and $\text{Ni}^{(\text{II})}$ -Hm complexes, (even in the presence of other amines) which can be oxidized and provides the low resolution peak at 600 mV. Relatively high concentrations of histamine leads to its adsorption to the anode and causes the second signal's potentials to shift to the higher values ($> 800 \text{ mV}$).

Histamine commercial product (70 mM) and $\text{NiSO}_4 \cdot 6\text{H}_2\text{O}$ (10 mM) were added to the suspension ($S_{\text{mix/fish}}$) and the resulting mixture was centrifuged, the solid removed, then the liquid fraction was analyzed. The obtained I/E curve (7, Figure 10), shows a peak centered at 598 mV, followed by a shoulder starting at $\sim 700 \text{ mV}$. The obtained signal for the $\text{Ni}^{(\text{II})}$ -Hm complex shows sat-

isfactory resolution for the concentration ratio ($[\text{Hm}]/[\text{Ni}^{(\text{II})}] = 7$) and higher current magnitude (in comparison with curve 6).

Comparison of the potentials of the previous signals (curve 6, wave from 400 to 750 mV and also curve 5: shoulder from 500 to 660 mV) with the potential (0.72 V curve 8) of the peak of signal obtained with the fish exposed to the sun, enables the conclusion that this signal corresponds to the oxidation of the $\text{Ni}^{(\text{II})}$ -Hm complex. Indeed oxidation of the $\text{Ni}^{(\text{II})}$ -Hm complex, in the fish mixture, starts at the same potentials to those of the signals of curves (6) and (7). The viscous nature of the matrix of the extracted and analyzed sample of fish (electrolyte/solvent/various solutes), could easily explain the minor differences in the peaks potentials. Moreover, low content of $\text{NiSO}_4 \cdot 6\text{H}_2\text{O}$ requires to operate with potential scan rates lower than 0.3 mV/s, to allow the chemical reaction (9) to take place and to regenerate the Ni 'catalyst'.

Note that the first signal shown in curve 8 (0.34 V) could be due to the presence in this fish of other biogenic amines (putrescin/1,4-diaminobutane, cadaverin/1,5-diaminopentane,...) probably able to form complexes, which could oxidize at these lower potentials. Nevertheless the signal was well separated from the second one and does not cause any disturbance.

Simple comparison of the peak magnitudes (curve 7, peak at 0.59 mV, $I_{\text{peak}} = 1.11 \mu\text{A}/\mu\text{L}$ and curve 8, peak at 598 mV, $I_{\text{peak}} = 2.3 \mu\text{A}/\mu\text{L}$) allows the concentration of histamine in the sun exposed fish to 148 mM to be estimated. Note that, with commercial histamine the lowest concentration of histamine, allows to obtain a nicely resolute signal, is in the range of 1 mM (curve 3 Figure 2: $0.6 \mu\text{A}/\mu\text{L}$).

This value is lower than the maximum admitted value of Histamine in the fish (200 mg of Hm/kg of fish \rightarrow 1.8 mM of Histamine) and open possibilities of direct analysis of fish without dilution. Nevertheless, low contents of Histamine in the fish must be investigated to define the lower concentration detected in the real matrix and directly in the fish.

Through the design of a simple nickel containing sensor, by simple and optimized measurements of the current, an estimation of the histamine content within the fish, will constitute the objective of future studies.

5 Conclusions

In this study, classical electrochemical thin layer measurements were carried out in order to understand the mechanism of the histamine indirect anodic oxidation, catalyzed by nickel sulfate in alkaline media. Results clearly show the evidence that histamine can complex the $\text{Ni}^{(\text{II})}$ and complete dissolution of nickel sulfate in 0.044 M NaOH media was observed for concentration ratios $[\text{Hm}]/[\text{Ni}^{(\text{II})}]$ higher than 3. The estimated equilibrium constant of this reaction is close to 10^6 order magnitude showing an important affinity of histamine to nickel.

The resulting complex (Ni^(III)-histamine) can be oxidized, in a single electron reaction, to Ni^(III)-histamine, which decomposes (9) to regenerate Ni^(III) and hydroxylated histamine. In this case the system Ni^(III)/Ni^(III) acts as an indirect redox mediator for histamine complete oxidation. This chemical reaction is slow ($k' = 4.5 \times 10^{-8} \text{ m}^3 \text{ mol}^{-1} \text{ s}^{-1}$) and is responsible of the observed 'no linearity' in the evolution of the peak current versus concentration and potential scan rate.

Results' reproducibility ($\Delta I_{\text{peak}} < 5\%$) was validated by three different plots for each parameter study, thus enabling validation of the proposed mechanism. Effect of the pH was not studied at the present study because in previous works [19] Švarc-Gajić and al evokes easy oxidation of Nickel hydroxide to nickel peroxide in alkaline media. Nevertheless the effect of the pH will systematically be studied in the near future, in order to examine consequences on the resulting Hm/Ni complex, as well as the rate of the chemical reactions (reduction of Ni(III) simultaneously to the oxidation of the histamine) because the possible ionization of the histamine in neutral or acidic media.

This method was applied to analyze extracts from fresh fish previously exposed to the sun for two days. High content of histamine (>0.1 M) was detected and this results shows potentialities to design a sensor for direct histamine measurement in fish. Future work will be devoted to the study of a simple electrode containing nickel sulfate (as catalyst) gel in the appropriate media in order to optimize the detection and to establish the required correlations between the histamine content and the operating parameters.

4 Nomenclature

C Concentration (M or mol L⁻¹),
E, *E*^o, *E*_{i=0} Potential, apparent standard potential and open circuit potential (V),
F Faraday's constant (96480 C mol⁻¹)
Hm histamine
I, *I*_{peak} current, peak current (A)
k^o, *k*^o apparent intrinsic, and intrinsic heterogeneous electronic transfer constants (ms⁻¹)
k and *k*' chemical reaction rate constant and chemical reaction apparent rate constant
K equilibrium constant
*n*_{over} the exchanged electron number for the overall process
*n*_{ls} or *n*_{lim step} the exchanged electron number for the limiting step (most often 1 e⁻)
R ideal gas constant (8.31 J mol⁻¹ K⁻¹)
r potential scan rate (Vs⁻¹ or mV min⁻¹)
S working electrode geometrical surface (m²)
T temperature (°C) and/or Absolute temperature (K)
t time (s)
*V*_{TL} thin layer cell volume (μL)
α anodic electronic transfer coefficient

Acknowledgements

We would like to thank Prof. *M. Comtat* (LGC UPS) for helpful discussions.

References

- [1] A. Askar, H. Treptow, *Amines, in Encyclopaedia of Food Science, Food Technology and Nutrition*, Academic Press, New York **1993**.
- [2] M. Lehane, J. Olley, *Int. J. Food Microbiol.* **2000**, *58*, 1.
- [3] J. E. Stratton, R. W. Hutkings, S. L. Taylor, *J. Food Protect.* **1991**, *54*, 460.
- [4] J. H. Hotchkiss, R. A. Scanlan, L. M. Libbey, *J. Agric. Food Chem.* **1977**, *25*(5), 1183.
- [5] H. Treptow, A. Askar, *Ernährung/Nutrition* **1990**, *14*, 9.
- [6] P. A. Lerke, L. D. Bell, *J. Food Sci.* **1976**, *4*, 1282.
- [7] I. Lange, K. Thomas, C. Wittmann, *J. Chromatograph. B* **2002**, *779*(2).
- [8] B. Kutlan, P. Presits, I. Molnar-Perl, *J. Chromatograph. A* **2002**, *949*(1–2), 235.
- [9] J. L. Mietz, E. Karmas, *J. Assoc. Off. Anal. Chem.* **1978**, *61*, 139.
- [10] AOAC Official Methods 977.13, in *Official Methods of Analysis of AOAC International*, 17th ed., AOAC International **2000**, ch. 35.
- [11] W. R. Staruszkiewicz, E. M. Waldom, J. F. Bond, *Anal. Chem.* **1977**, *60*, 1125.
- [12] V. Frattini, C. Lionetti, *J. Chromatogr. A* **1998**, *809*(1–2) 241.
- [13] J. Y. Hui, S. L. Taylor, *Toxicol. Hypl. Pharmacol.* **1985**, *8*, 241.
- [14] R. Drasci, L. Giannetti, P. Boria, L. Lucentini, L. Palleschi, S. Cavalli, *J. Chrom. A.* **1998**, *798*, 109.
- [15] I. G. Casella, M. Gatta, E. Desimoni, *Food Chem.* **2001**, *73*, 367.
- [16] I. G. Casella, T. R. Cataldi, A. M. Salvi, E. Desimoni, *Anal. Chem.* **1993**, *65*, 3143.
- [17] R. P. Deo, N. S. Lawrence, J. Wang, *Analyst* **2004**, *129*, 1076.
- [18] I. Danaee, M. Jafarian, F. Farouandeh, F. Gobal, M. G. Mahjani, *Int. J. Hydrogen Energy* **2008**, *33*(16), 4367.
- [19] J. Švarc-Gajić, Z. Stojanović, *Electroanalysis* **2010**, *24*, 2931.
- [20] K. Takagi, S. Shikata, *Anal. Chim. Acta* **2004**, *505*(2), 189.
- [21] A. Dalmia, C. C. Liu, R. F. Savinell, *J. Electroanal. Chem.* **1997**, *430*, 205.
- [22] R. H. Patil, R. N. Hegde, S. T. Nandibewoor, *Colloids Surf. B, Biointerf.* **2011**, *83*, 133.
- [23] B. V. Sarada, T. N. Rao, D. A. Tryk, A. Fujishima, *Anal. Chem.* **2000**, *72*, 1632.
- [24] T.-K. Lim, H. Ohta, T. Matsunaga, *Anal. Chem.* **2003**, *75*, 3316.
- [25] J. A. Young, X. Jiang, J. R. Kirchoff, *Electroanalysis* **2013**, *25*(7), 1589–1593
- [26] M. Comtat, H. Durliat, *Biosens. Bioelectron.* **1994**, *9*(9–10), 663–668.
- [27] T. V. Shishkanova, G. Broncova M. Kronak, D. Sykora, V. Kral, *J. Mater. Sci.* **2011**, *46*, 7594–7602.
- [28] D. Miller, H. Sanchez-Casalogue, H. Bluhm, H. Ogawara, A. Nilsson, S. Kaya, *J. Am. Chem. Soc.* **2014**, *136*, 6340–6347.
- [29] N. Seriani, Z. Jin, W. Pompe, L. Colombi Ciacchi, *Phys. Rev. B* **2007**, *76*, 155421.
- [30] R. K. Nomiya, M. J. Piotrowski, L. F. DaSilva, *Phys. Rev. B* **2011**, *84*, 100101(R).

- [31] B. Trémillon, *Electrochimie Analytique et Réactions en Solution*, Wiley, Chichester **1997**.
- [32] A. J. Bard, L. R. Faulkner, *Electrochemical Methods. Fundamentals and Applications*, 2nd ed., Wiley, New York **2001**.
- [33] P. Drozdowski, E. Kordon, *Spectrochim. Acta A* **2000**, 56, 2459–2464.
- [34] Y. Altun, F. Koseoglu, *J. Solution Chem.* **2005**, 34(2).
- [35] J. A. Arias-Montafio, J. M. Young, *Eur. J. Pharmacol. – Mol. Pharmacol.* **1993**, 245, 221–228 221.
- [36] P. R. Reddy, N. Raju, K. S. Rao, A. Shilpa, *Ind. J. Chem.* **2009**, 48A, 761–768.
- [37] J. E. Stratton, R. W. Hutkins, S. L. Taylor, *J. Food Protect.* **1991**, 54, 460.
- [38] P. A. Lerke, L. D. Bell, *J. Food Sci.* **1976**, 41, 1282.
-